An analysis for the effect of nozzle losses on the air-cushion pressure parameter accounted for a substantial portion of the difference between theory and experiment for those models for which the length-to-width ratio effects were small. The analysis also predicted a Reynolds number variation in agreement with experiment.

The hover tests indicated that the presence of an encapsulating shell about the air cushion generally deteriorated its performance at low cushion heights.

The forward-speed tests indicate that a moving-ground plane probably is needed for acceptable wind-tunnel results.

In general, the moving ground induced a positive longitudinal pressure gradient on the cushion base which contributed a negative pitching moment to the cushion. This characteristic was qualitatively verified by an approximate theoretical analysis of the effect of ground-plane motion on the cushion-bottom flow.

At forward speed, the moving ground was responsible for cushion lift increases in excess of the hover lift, the exact magnitude of the increase being dependent on cushion mode and the magnitude of the hover lift. In general, the cushion lift increased with forward speed until a peak value was reached.

For further increases in speed, the lift diminished with speed, but generally remained above the hover lift for most of these tests. This characteristic diminished with increasing height. For speeds below the peak lift, the moving ground was responsible for a major portion of the lift increase, although some contribution was obtained from the airstream. For speeds above the peak lift, the airstream was responsible for diminishing the lift.

For the single cushion elongated model utilizing both hybrid-plenum and peripheral-jet cushions, the hybrid-plenum cushion tended to perform like the peripheral one although there is not a well-defined pattern of behavior for the hybrid case. For speed parameter values below 1.4, the hybrid-plenum cushion required the lesser total power, whereas for speed-parameter values above 1.4, the reverse was true.

For the single cushion elongated model, with cushion power off, the body lift coefficient is relatively independent of whether the ground plane is moving or stopped. With cushion power on and the ground plane moving, however, a large loss in lift occurs at low values of the forward-speed parameter. It is hypothesized that the lift degradation is caused by the cushion forward efflux dominating the flow at the low forward speed. That is, the cushion is operating in what is commonly called the subcritical flow regime.

For elongated vehicles, the body forces and moments generally dominate over those of the cushion for all characteristics but the lift and pitching moment. Near zero yaw angle, for the ground plane moving, the cushion lift and pitching moment dominate, whereas at the higher yaw angles, the body lift dominates, and the cushion and body pitching moments are usually equally influential.

References

[1] Woolard, H. W., So, K. L., and Sergeant, R. J., "Moving Ground-Plane Wind-Tunnel Tests on Several Tracked Air Cushion Vehicle (TACV) Models," TRW Rept. 06818-6032-RO-00, March 1969, Redondo Beach, Calif. (PB 183857).

[2] Turner, T. R., "A Moving-Belt Ground Plane for Wind-Tunnel Ground Simulation and Results for the Two Jet-Flap Configurations," TN D-4228, Nov. 1967, NASA.

[3] Grunwald, K. J., "Aerodynamic Characteristics of High Fineness Ratio Vehicle Bodies at Cross-Wind Conditions in Ground Proximity," Working Paper 490, Oct. 10, 1967, NASA Langley.

[4] Woolard, H- W., "Slender-Body Aerodynamics for High-Speed Ground Vehicles," AIAA Paper 70-139, New York, 1970.

[5] Walker, N. K., "Some Notes on the Lift and Drag of Ground Effect Machines," *Proceedings of the National Meeting on Hydrofoils and Air Cushion Vehicles*, Institute of Aerospace Sciences, 1962.

JUNE 1971 J. AIRCRAFT VOL. 8, NO. 6

Graphite-Epoxy Wing for BQM-34E Supersonic Aerial Target

EDWARD J. MCQUILLEN* AND SHIH L. HUANG†
Naval Air Development Center, Warminster, Pa.

A graphite-epoxy composite wing has been analytically synthesized and designed. The objectives of this program were to exploit the improved properties of advanced fiber reinforced composites for primary structure of high-performance airborne vehicles, to extend structural mechanics technology to these nonisotropic, nonhomogeneous materials, and to gain service experience with no risk to human life. A computerized iterative design-analysis approach was used to minimize weight subject to both strength and flutter constraints. The wing is of sandwich construction with graphite-epoxy laminate skins bonded to aluminum honeycomb. The weight reduction was 50%.

Nomenclature

a_i = thermal expansion coefficient; $i = 1,2,6$
C_{ij} = stiffness matrix element; $i,j = 1,2 \ldots 6$
EI = bending rigidity
GJ = torsional rigidity
$h_L^{(k)}$ = distance from midplane to lower surface of kth ply
$h_u^{(k)}$ = distance from midplane to upper surface of kth ply
I = section mass moment of inertia
K_i = bending and torsional curvature of laminate; $i = 1,2,6$
M = mass
M_i = stress couple; $i = 1,2,6$
N_i = stress resultant; $i = 1,2,6$
n = total number of plies

Presented at the AIAA/ASME 11th Structures, Structural Dynamics, and Materials Conference, Denver, Colo., April 22–24, 1970; submitted May 21, 1970; revision received November 23, 1970. This paper represents results of in-house effort under Independent Research. Acknowledgment is made to the other members of the Applied Mechanics Research Group at the Naval Air Development Center who participated in this program. In particular A. Somoroff and T. Neu and H. Rubin made substantial contributions to the over-all effort.

* Head, Applied Mechanics Research Group, Aeromechanics Department. Member AIAA.
† Aerospace Engineer, Applied Mechanics Research Group, Aeromechanics Department.

Q_{ij} = plane-stress stiffness element; i,j = 1,2,4,5,6
S = mass unbalance
S_{ij} = compliance matrix element; i,j = 1,2,4,5,6
T = temperature
T_{ij} = stress transformation matrix element; i,j = 1,2,6
T_{ijkl} = stiffness transformation matrix; i,j = 1,2,4,5,6; k,l = 1,2,4,5,6
t = thickness of the laminate
X_i = longitudinal, transverse and shear ultimate stresses; i = 1,2,6
Z = distance from midplane of the laminate
ϵ_i = strain; i = 1,2 . . . 6
ϵ_{0i} = midplane strain; i = 1,2,6
σ_i = stress; i = 1,2 . . . 6
ρ = mass of the wing per unit length

Superscripts and subscripts

G = wing with graphite-epoxy face sheets
(k) = kth ply
S = wing with steel face sheets

Introduction

THE Naval Air Development Center has synthesized and designed a graphite-epoxy wing for the unmanned BQM-34E supersonic aerial target vehicle. This was a completely in-house effort under Independent Research. It is planned to fabricate several complete wing assemblies. One will be used for laboratory static and vibration tests and the others for flight tests. The objectives of this effort are to exploit the improved material properties of the new filament composites, to extend structural mechanics technology to these nonhomogeneous, nonisotropic materials, to develop an optimum design with minimum weight, to demonstrate its use, and to obtain service experience on a primary structural component of a high performance vehicle with no risk to human life.

Among the various advanced composite materials, graphite-epoxy composite, exhibiting high strength and high stiffness coupled with low density, is very attractive for many aerospace structural applications.

The two most significant characteristics of the composite materials from the designer's standpoint are 1) the improved properties—higher strength/density and higher stiffness/density; and 2) the directionality of the material. Unlike conventional isotropic metals whose properties are invariant regardless of direction, the composite materials are much stronger and stiffer in the direction of the reinforcing filaments—they are anisotropic.

When a new material such as an advanced composite is made available it becomes the task of the structural designer and the structural analyst to make the most efficient utilization of the improved material properties in applications.

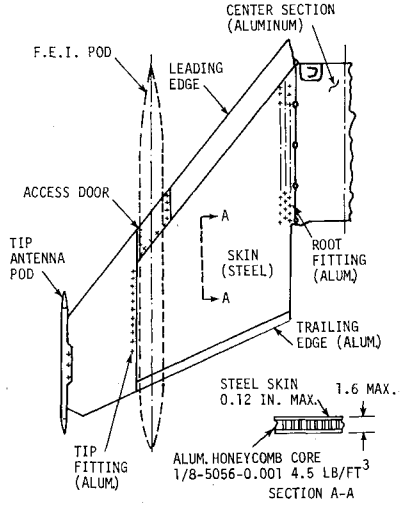

Fig. 1 Original BQM-34E steel wing.

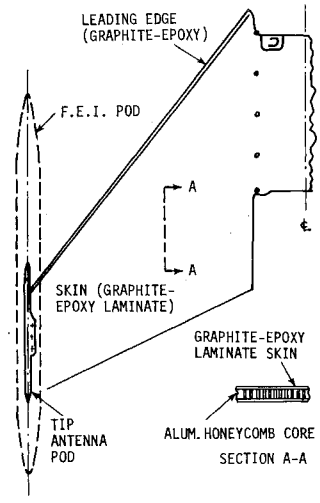

Fig. 2 BQM-34E composite wing.

On the one hand the anisotropy and nonhomogeneity of the new composite materials complicate the task of the structural analyst; but on the other hand, because of their directionality they also provide new degrees of freedom to the designer, i.e., the possibility of tailoring the strength and stiffness precisely to the amount and in the direction required in a particular application. Structural optimization and weight minimization take on new meaning.

The subject aerial target is a turbo-jet powered, high altitude, supersonic, unmanned vehicle. The present wing, Fig. 1, is swept with moderate aspect and low thickness ratios. The main panel is constructed of stainless-steel skins bonded to a full-depth aluminum honeycomb. These skins are taper chem-milled to optimize the wing structure for stress and flutter.

In the composite wing design emphasis was placed on reducing the weight and the number of major subassemblies while maintaining the original airfoil shape and planform. Since the original design was flutter critical, the composite design has to satisfy both the strength and flutter criteria of the original wing.

The composite wing assembly, including the center section, consists of two identical halves joined along the centerline as shown in Fig. 2. The upper and lower surfaces of the wing are covered with graphite-epoxy laminate bonded to an aluminum honeycomb core. The leading edge is made of the same material and there is no separate trailing edge.

The center joint, shown in Fig. 3, involves both bonded and pin joints. The joint is skew symmetric to provide two identical and interchangeable halves. Special metal shims and bushings are provided at fuselage attachment points. These are designed for local load transfer and to reduce bearing stress and tear-out stress on the graphite composite skins.

The basic building block of the composite laminate skins is unidirectional tape, which is highly anisotropic. Effective utilization of the tape depends upon synthesis of a multidirectional composite laminate to satisfy both strength and stiffness requirements. This synthesis required the development of methods of computerized analysis based upon laminate theory.

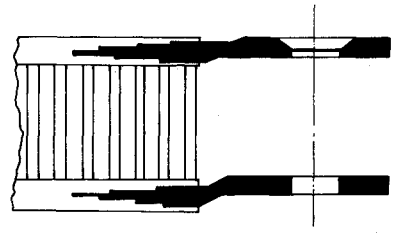

Fig. 3 Composite wing center joint.

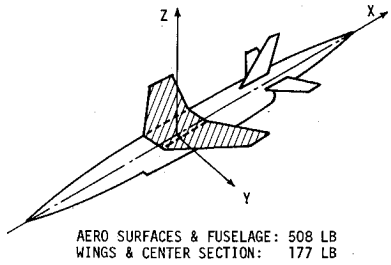

Fig. 4 BQM-34E vehicle configuration.

In order to achieve both mechanical and thermal balance, plies are arranged symmetrically with respect to the midplane of the laminate. This thermal balance is important because of the marked difference in coefficient of thermal expansion in directions longitudinal and transverse to the fibers. The skin thickness is tapered spanwise and chordwise by adding or eliminating plies. Modmor II graphite fiber-epoxy resin prepreg tape was found to be the most suitable material. Various composite materials and variable but balanced laminate lay-up constructions were analytically examined using the computer program developed for this purpose. A thickness distribution using this material was determined such that the structure would have the strength to carry (with a suitable margin of safety) the design loads of the original wing and in addition have the combination of stiffness and mass distribution required to prevent flutter throughout the flight envelope. The preliminary design was completed and a final, automated, iterative, analysis-design procedure was carried out. This procedure involves interaction of three separate types of analysis: 1) laminate analysis, 2) structural analysis, and 3) aeroelastic analysis.

In the preliminary design a reduction of approximately 50% of weight has been achieved. The graphite wing consists of two major subassemblies in lieu of the original five; and, in addition, can be field disassembled into two identical halves.

A laboratory test program was conducted. Small specimens were tested to verify the laminate strength and stiffness properties analytically predicted. It is planned to test small components to check design details and the strength of fasteners and attachments.

Flight testing of this composite wing will demonstrate the applicabiilty of composite materials to major structural elements of high-performance aerospace vehicles.

Design Criteria

General Description

The BQM-34E is a turbo-jet propelled, high-altitude, supersonic unmanned aerial target vehicle. This vehicle was developed under contract by the Naval Air Systems Command. The vehicle configuration has a swept-back wing and empennage. All surfaces are tapered in planform. There are no ailerons; roll control is achieved by means of differential deflection of the all-movable horizontal tail surfaces. The general configuration is shown in Fig. 4.

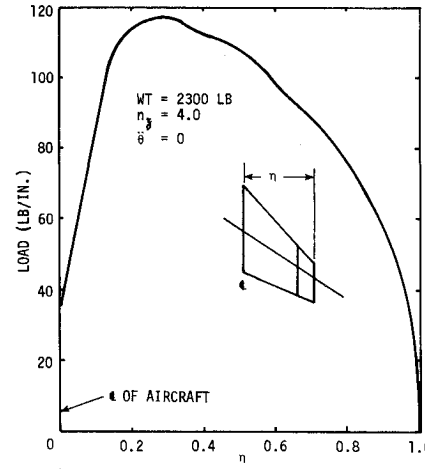

Fig. 5 BQM-34E limit spanwise aerodynamic loads, symmetric maneuver, $M = 0.55$.

The target vehicle can be air launched from a DP-2E aircraft or ground launched (zero length JATO). It is capable of turn, climb, and dive maneuvers upon command from ground or flight control stations. Upon completion of its mission, the vehicle is recovered with a two-stage parachute system. The vehicle descends on the main parachute and impacts on the ground or on water. Vehicle maximum gross weight is approximately 2300 lb.

This vehicle has a moderate aspect ratio, swept, honeycomb sandwich, slab type wing, representative of missile and aircraft lifting surfaces of low thickness ratio. The main wing panel is constructed of full-depth aluminum honeycomb core, bonded to stainless-steel facing sheets with low-temperature organic adhesive. The face sheets are taper chem-milled to optimize the structure for stress and flutter considerations. The wing tip is of full-depth fiber glass core and fiber glass face sheets bonded with low-temperature organic adhesive. A view of the original wing is presented in Fig. 1.

Criteria

The design criteria applied to the composite wing are those specified for the original wing. A summary of the structural design criteria is shown in Table 1. Since the most significant load acting on the wing is the aerodynamic load, the critical design condition is in free flight with high-g pull-up. The two most critical wing loading conditions are 4-g symmetric pull-ups at Mach 0.55 and 1.05. Spanwise aerodynamic loadings for these conditions are shown in Figs. 5 and 6. The composite wing must be flutter free within the entire flight envelope of the vehicle.

Analysis

Preliminary Analysis

Since flutter, as well as strength, was of primary consideration in the original design, the preliminary analysis was

Table 1 Summary of structural design criteria

Condition	Ultimate safety factor	Max. limit load factor n_x	Max. limit load factor n_y	Max. limit load factor n_z	Comment
Free flight					
Symmetric	1.25			$-2.0 \sim 4.0$	$\ddot{\theta} = 3$ rad/sec^2
Asymmetric				$1.0 \sim 3.2$	$U = 27$ fps
Captive flight					
DP2-E	1.50	± 2.5	± 1.5	$-3.0 \sim 6.0$	$U = 50$ fps
Recovery	1.25	12.5	± 3.0	6.0	
Ground loads	1.50	$-7.0 \sim 6.0$	$-1.5 \sim 3.0$	$-2.0 \sim 12.0$	
Water impact	1.25	± 3.0	± 4.0	7.5	

based upon matching the dynamic stiffness of the original design. By dynamic stiffness of the wing is meant the distribution, along the elastic axis of $(GJ/\rho)^{1/2}$ and $(EI/\rho)^{1/2}$ values (since the frequencies of vibration are dependent upon these values). Assuming the composite wing will weigh approximately half the original, then,

$$(EI/\rho)_G{}^{1/2} = (EI/\rho)_S{}^{1/2}, \quad (GJ/\rho)_G{}^{1/2} = (GJ/\rho)_S{}^{1/2}$$

Therefore, matching the dynamic stiffness requires the $(GJ)_G$ and $(EI)_G$ of the composite design to be half that of the original wing.

It also follows from the aforementioned that

$$(EI)_G/(GJ)_G = (EI)_S/(GJ)_S$$

which means that the ratio of the bending to torsional stiffnesses of the composite wing will be the same as the original wing. Various composite materials and variable laminate lay-up constructions were analytically examined. An optimum laminate skin matching the strength criteria and dynamic stiffness of the original design was synthesized. A preliminary detailed design was completed and a preliminary flutter analysis conducted. The results of the flutter analysis indicated modifications of stiffness and mass to improve dynamic aeroelastic response. These modifications were made, and the final design strength and flutter analyses were completed as discussed below.

Final Analysis

A final, automated, iterative analysis-design procedure as illustrated by the block diagram shown in Fig. 7, was conducted. The procedure requires three separate but coupled types of analysis: 1) laminate analysis; 2) structural analysis; and 3) dynamic aeroelastic analysis.

Each analysis requires a computer program. In addition, although not shown, an input data generation program was required. As shown there are two cycles, an inner stress analysis loop and an outer flutter loop. The procedure begins with the laminate analysis program. Wing geometry, orthotropic material properties, ply orientations, and skin thickness distribution from the preliminary design are the initial input. The laminate analysis program computes the element stiffness matrix for the idealized wing structure. These data with the external aerodynamic load distribution are inputs to the structural analysis program. This program computes internal load distribution, wing stiffness and mass properties in the proper matrix form required for the flutter analysis program, and natural frequencies and mode shapes of vibration. A flutter analysis is conducted using the results from the structural analysis. Comparison of computed flutter speeds with the required performance of the vehicle

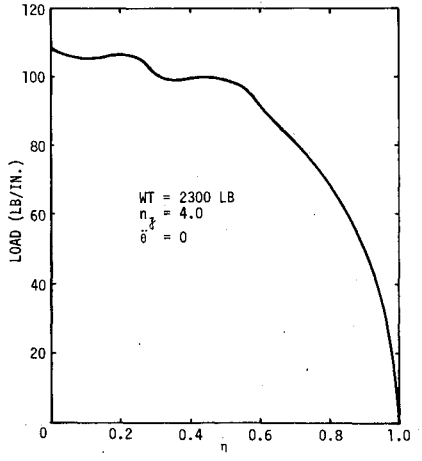

Fig. 6 BQM-34E limit spanwise aerodynamic loads, symmetric maneuver, $M = 1.05$.

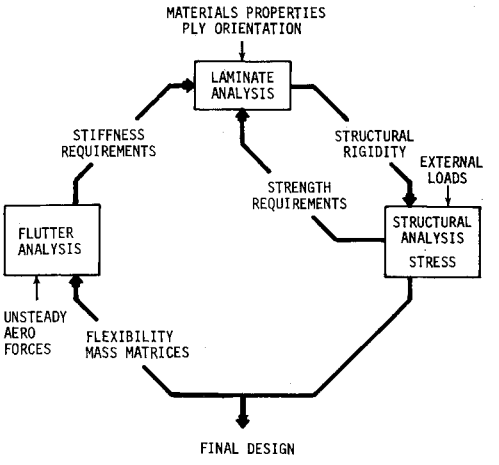

Fig. 7 Over-all analysis cycle.

determines whether design modification of stiffness and/or mass properties is required.

Each of the three types of analysis and the iterative analysis cycles are discussed below.

1. Laminate analysis

Approximately 80% of the weight of the original wing is in the skins which will be replaced by graphite-epoxy laminate. The success of minimizing the structural weight of the wing, therefore, depends largely on the efficient design of the laminate to meet local strength and stiffness requirements.

The basic building block of the laminate is unidirectional tape. The laminate consists of many plies of the tape. The designer is provided freedom in the following choices: 1) the basic tape properties and tape thickness; 2) the lay-up sequence, the angular orientation of each ply, and local laminate thickness (number of plies); and 3) the curing cycle.

Laminate theory is presented in Refs. 1 and 2 and is summarized below. The unprimed coordinate system refers to each of the individual plies while the primed system refers to the principal axes of the laminate.

In the formulation of a theory to predict laminate properties from tape properties, it is first assumed that transverse normal stress is negligible in the laminate. If the stress-

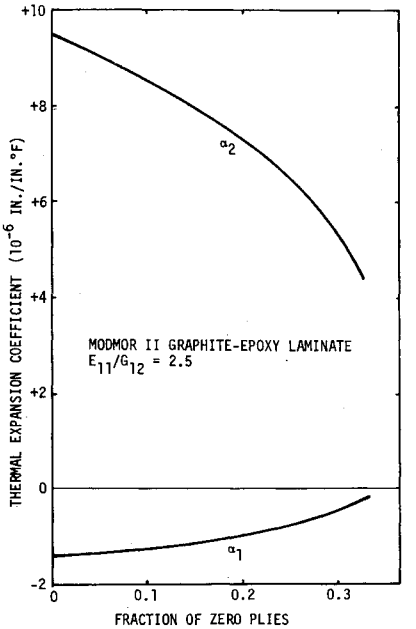

Fig. 8 Laminate thermal expansion coefficients.

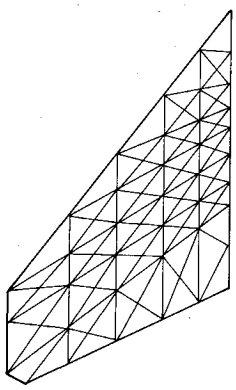

Fig. 9 Schematic of triangular plate structural idealization.

strain equations for the unidirectional composite are written as

$$\epsilon_i = S_{ij}\sigma_j, \quad \sigma_i = C_{ij}\epsilon_j$$

and the assumption that $\sigma_3 = 0$ is inserted, then

$$\epsilon_i = S_{ij}\sigma_j \qquad i,j = 1,2,4,5,6$$
$$\sigma_i = Q_{ij}\epsilon_j \qquad i,j = 1,2,4,5,6$$

where

$$Q_{ij} = C_{ij} - C_{i3}C_{3j}/C_{33}$$

If the fibers are oriented at an angle to the principal axis of the laminate then the plane-stress stiffness coefficients are transformed by the relation

$$Q_{ij}' = T_{ijkl}Q_{ke}$$

Because of the orthotropic nature of the unidirectional composite,

$$Q_{16} = Q_{26} = Q_{14} = Q_{15} = Q_{25} = Q_{25} = Q_{64} = Q_{65} = Q_{45} = 0$$
$$Q_{14}' = Q_{15}' = Q_{24}' = Q_{25}' = Q_{64}' = Q_{65}' = 0$$

The equations relating $\sigma_4,\sigma_5,\epsilon_4,\epsilon_5$ are independent of those relating $\sigma_1,\sigma_2,\sigma_6,\epsilon_1,\epsilon_2$, and ϵ_6; and are not needed in this theory. There remain only three equations relating σ_1, σ_2,σ_6 and $\epsilon_1,\epsilon_2,\epsilon_6$.

Once the individual plies have been bonded to form the laminate, there is placed on the laminate an additional constraint, that there be no relative displacement between the contiguous surfaces of the plies and that normals to the midplane remain normal. Employing this constraint, the strain in any ply is expressed by

$$\epsilon_i'^{(k)} = \epsilon_{0i}' + K_i'Z$$

If strains and curvatures are applied to the laminate, stresses will be induced in each ply in proportion to its stiffness;

$$\sigma_i'^{(k)} = Q_{ij}'^{(k)}\epsilon_j'^{(k)} = Q_{ij}'^{(k)}(\epsilon_{0j}' + K_j'Z) - Q_{ij}'^{(k)}a_j'T$$

Assuming that each ply is macroscopically homogeneous, by integrating the stresses over the total thickness of the laminate, the stress resultants N_i and distributed bending moments M_i are related to the curvatures and midplane strains as follows:

$$N_i = A_{ij}\epsilon_{0j}' + B_{ij}K_j' - \int_{-t/2}^{t/2} Q_{ij}'^{(k)}a_j'^{(k)}TdZ$$

$$M_i = B_{ij}\epsilon_{0j}' + D_{ij}K_j' - \int_{-t/2}^{t/2} Q_{ij}'^{(k)}a_j'^{(k)}TZdZ$$

where

$$A_{ij} = \sum_{k=1}^{n} Q_{ij}'^{(k)}(h_u^{(k)} - h_L^{(k)})$$

$$B_{ij} = \frac{1}{2}\sum_{k=1}^{n} Q_{ij}'^{(k)}[(h_u^{(k)})^2 - (h_L^{(k)})^2]$$

$$D_{ij} = \frac{1}{3}\sum_{k=1}^{n} Q_{ij}'^{(k)}[(h_u^{(k)})^3 - (h_L^{(k)})^3]$$

From these expressions, it is seen that if the basic lay-up construction is symmetric about the midplane and if there are an equal number of plus and minus angular plies then the laminate is balanced. There is no coupling between stress resultants and curvatures, or between stress couples and inplane strains. Also the normal stress resultants are a function of normal strain only. There is thermal balance in that there is no warping when the composite is at a temperature different from the curing temperature. There is, however, coupling between bending and twist. In the present case where the laminate forms the facing of a sandwich construction, the laminate bending is very small, and this coupling is negligible. In the design of the laminate this basic balanced laminate was used. As a result

$$B_{ij} = 0, \quad A_{16} = 0, \quad A_{26} = 0$$

and

$$\int_{-t/2}^{t/2} Q_{6j}'^{(k)}a_j'^{(k)}TdZ = 0$$

In the search for an optimum basic laminate construction, thermal effects can be omitted thus,

$$N_i = A_{ij}\epsilon_{0j}' \quad \text{and} \quad M_i = D_{ij}K_j'$$

To find the strength of the laminate, it is first necessary to calculate the stresses in individual plies. By inverting the A and D matrices, the midplane strain and curvature may be found by the following relations:

$$\epsilon_{0i}' = A_{ij}^{-1}N_j, \quad K_i' = D_{ij}^{-1}M_j$$

Therefore,

$$\epsilon_i'^{(k)} = A_{ij}^{-1}N_j + ZD_{ij}^{-1}M_j \quad \text{and}$$
$$\sigma_i'^{(k)} = Q_{ij}'^{(k)}(A_{ji}^{-1}N_i + ZD_{ji}^{-1}M_i)$$

The stresses found for each ply are then transformed into the tape coordinate system by

$$\sigma_i^{(k)} = T_{ij}^{(k)}\sigma_j'^{(k)}$$

In general, all three stresses, σ_1, σ_2, and σ_6 will occur in each ply, and some criterion must be used to determine whether such a state of combined stress is allowable.

Though a number of strength criteria have been proposed, one which is prominent, partly because it is conservative in

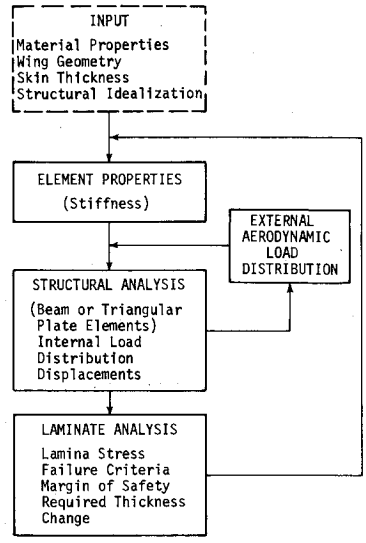

Fig. 10 Strength analysis cycle.

Table 2 Estimated properties of the unidirectional tape and analytically predicted properties of the laminate

	Unidirectional material		Laminate	
	MFG estimate	Measured	Anal. pred.	Measured
E_{11}	20×10^6 psi	20×10^6 psi	8.13×10^6 psi	8.07×10^6 psi
E_{22}	1.2×10^6 psi	1.5×10^6 psi	3.00×10^6 psi	2.40×10^6 psi
G_{12}	0.9×10^6 psi		3.25×10^6 psi	
V_{12}	0.27	0.25	0.72	0.82
X_1	130 ksi	125 ksi	56.6 ksi	55.6 ksi
X_2	8 ksi	5.5 ksi	22.3 ksi	21.5 ksi
X_6	11 ksi		39.8 ksi	
SBS	15 ksi	15 ksi	15 ksi	13 ksi

cases of combined stress, is the Von Mises criterion. For an anistropic material subject to plane stress, it is expressed as

$$\left(\frac{\sigma_1}{\sigma_{1a}}\right)^2 - \frac{\sigma_1\sigma_2}{\sigma_{1a}{}^2} + \left(\frac{\sigma_2}{\sigma_{2a}}\right)^2 + \left(\frac{\sigma_6}{\sigma_{6a}}\right)^2 \leq 1$$

Since the material does not have definable yield points, the allowable stresses, $\sigma_{1a},\sigma_{2o},\sigma_{6a}$ in the above equation were set equal to the ultimate strengths X_1,X_2,X_6 of the composite divided by a suitable factor.

In order to find specific combinations of lay-up angles for a laminate having the proper stiffness ratio, computer programs were written to find the lay-up angles and the properties of the equivalent homogeneous material, and to determine the ultimate values of average stresses $\bar{\sigma}_i$ which may be applied to the laminate such that the Von Mises criterion is satisfied for each ply. In view of practical considerations, particularly simplicity and achievement of balanced construction with a minimum number of plies, the search was limited to only three angles, 0, $\pm\alpha$, $\pm\beta$. In each case, the zero plies represent some fraction of the total number of plies, while the remainder is divided evenly between those oriented at $\pm\alpha$ and $\pm\beta$. It may be shown by analysis and verified by calculations that maximum stiffness of a laminate is attained when $\alpha = \beta$ and a large portion of zero plies is used.

Various composite materials and ply orientations were analytically compared using the computer program developed for this purpose.

Modmor II graphite-epoxy resin prepreg tape was found to be the most suitable material and the optimized laminate construction consists of equal numbers of zero degree, $+42°$ and $-42°$ plies.

Estimated properties of the unidirectional tape and analytically predicted properties of the laminate are presented in Table 2.

A laboratory test program was conducted using small specimens. Experimentally measured properties of the unidirectional and angle ply laminates are shown for comparison. It is seen that good correlation was obtained. Longitudinal and transverse thermal expansion coefficients of the laminate for various fractions of zero plies are shown in Fig. 8. It is noted that the transverse laminate expansion coefficient for one-third zero plies is close to that of titanium which is used for inserts and joints.

2. *Structural analysis*

The geometry of the wing is too complex for the successful use of closed form analytical techniques. Therefore numerical analyses were used. Since an iterative design procedure is involved there is advantage to having structural idealizations of varying levels of complexity. To reduce the amount of input data generation and to facilitate computer turn around time an approximate elastic-axis beam representation was utilized for the initial flutter iterations. An orthotropic beam element representation was employed for the initial determination of internal load distribution and laminate stresses. The final structural analysis was based upon an orthotropic triangular plate finite element idealization. These elements and the computer program formulations are described in Refs. 3 and 4. The elastic axis representation is applicable for determining structural influence coefficients for wings of moderate aspect ratio. It is consistent with the incompressible strip theory aerodynamics employed in the initial flutter analyses.

Figure 9 shows a schematic of the structural idealizations used in the triangular plate element program. The strength analysis cycle is illustrated schematically in Fig. 10. The finite-element structural idealization, wing geometry, orthotropic material properties, and skin thickness are input to an element properties program which computes the stiffness properties of all the elements. These results provide the required input for the finite-element structural analysis program which computes for the purpose of this cycle internal load distribution and deflections. A separate closed inner loop is provided for the external aerodynamic load distribution to account for static aeroelastic effects. The internal load distribution is input to a laminate analysis program which computes stresses in individual plies of the laminate, applies a combined stress failure criteria and computes a margin of safety at each nodal point. The local thickness modification required to change the margin of safety to the desired value was calculated. The output of each program is in the form of punched cards with data in the correct format for use as input for the next program. Manual intervention and engineering judgment are required at each interface. Since the strength analysis loop and the flutter analysis loop are separate it is necessary for the analyst to decide at each interface if the strength or flutter requirement is critical at a particular wing section. A final thickness distribution was determined to satisfy both strength and flutter requirements. The skins have a linear thickness taper from the trailing edge perpendicular to the elastic axis. This taper was to provide the best combination of mass balance, overall section stiffness and local load carrying capability. Final iterations using the orthotropic triangular plate idealization were conducted using a finer mesh pattern in the fuselage attachment region to obtain a more accurate determination of the local stress concentration.

3. *Flutter analysis*

The original wing was flutter critical, and required the use of stainless-steel skins to obtain the necessary stiffness and mass balance to prevent flutter in the low altitude high-speed flight regime. The initial flutter analysis for the composite design was conducted using a collocation program described in Ref. 5. The flutter analysis cycle is illustrated schematically in Fig. 11. In order to determine the aeroelastic behavior of the wing it was necessary to compute the unsteady aerodynamics, the elastic properties, and the mass distribution of the structure. The initial flutter iterations were based upon aerodynamic influence coefficients computed using Theodorsen's incompressible strip theory as described in Refs. 6 and 7. The simplest approach to the problem of determining the structural deformation characteristics of the wing is to make the assumption that the

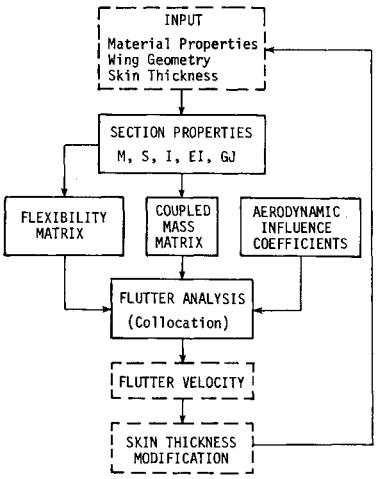

Fig. 11 Flutter cycle.

structure bends and twists as if it were a beam located along the elastic axis. This elastic axis idealization was used for the calculation of the structural influence coefficients which are compatible with strip theory aerodynamics. These computations were made using a program described in Ref. 8. The analysis is based upon elastic energy principles. The input for the program is simply the distribution of bending and torsion stiffness along the elastic axis. A program was prepared to compute wing section properties (EI, GJ, M, S, and I) for a given material and wing geometry (including skin thickness).

It was necessary to find the mass matrix corresponding to the chosen collocation points. A coupled mass matrix program (which required as input the inertial properties as total weight, center of gravity location and moments of inertia of chordwise sections) was prepared for this purpose. These data are transformed into an equivalent system of lumped masses. The aerodynamic, elastic, and inertial properties of the wing are input to the collocation flutter analysis program and a flutter speed is determined for each altitude.

The advantage of the simplified elastic representation in the initial iterations was that meaningful parametric comparisons could be conducted. The gross section stiffnesses (EI and GJ) and mass properties (M,S,I) which have physical meaning to the designer were changed, one at a time. The variation in flutter speed was then intuitively related to changes in the gross properties. This information was the basis of engineering judgment exercised in interpreting results of one iteration in terms of modification for the next cycle. Thus a semi-intuitive, iterative, weight minimization was carried out subject to strength, local buckling, and both static and dynamic aeroelastic constraints. The final design was analyzed for strength and flutter using a more accurate orthotropic triangular plate structural idealization and compressible aerodynamic influence coefficients based upon lifting surface techniques described in Refs. 9 and 10. Figure 12 presents the flutter characteristics at sea level of 1) the original steel wing; 2) the preliminary graphite design, based upon matched dynamic stiffness as described earlier, and 3) the final design. It is noted that although the preliminary composite design matched the first bending and torsional frequencies of vibration of the original wing within five percent, the flutter speed was approximately 100 knots lower. The flutter speed of the final design was increased to the required value primarily by moving mass forward in the outer half of the wing. The section c.g. location was shifted forward by means of a linear chordwise skin thickness taper.

Conclusions

The steel facings of the BQM-34E supersonic, aerial target can be replaced by laminated graphite-epoxy which provides

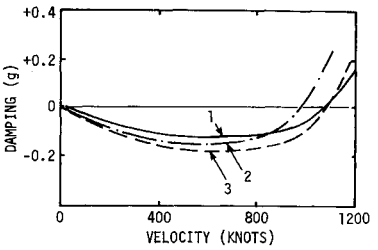

Fig. 12 Flutter characteristics at sea level.

equivalent strength and flutter behavior with a weight saving of approximately 50%.

An optimum laminate construction having the required multidirectional stiffness and strength, simplicity, and minimum balanced thickness has been synthesized using a zero, $\pm 42°$ lay-up with one-third zeros.

Laboratory laminate specimen tests have experimentally confirmed the analytically predicted stiffness and strength of the selected basic laminate construction.

A linear skin thickness taper in the chordwise direction was required to obtain a mass distribution to satisfy flutter requirements. This was easily achieved by adding or dropping plies in the composite laminate skin.

The composite wing assembly consists of two identical and interchangeable halves joined along the centerline. These two halves, which can be field assembled, are in lieu of five factory assembled subassemblies in the original steel wing. The upper and lower surfaces of the wing are covered with graphite-epoxy laminate bonded to an aluminum honeycomb core. The leading edge is made of the same material and there is no separate trailing edge.

It is planned to fabricate wing assemblies for static and vibration laboratory tests and for full scale flight tests. Operational flight testing of this composite wing on a high-performance vehicle will provide service experience for a primary composite airframe structure with no risk to human life.

References

[1] Tsai, S. W., "Mechanics of Composite Materials," TR AFML-TR-66-149, Pt II, Nov. 1966, Air Force Materials Lab.

[2] Dong, S. B., Pister, K. S., and Taylor, R. L., "On the Theory of Laminated Anisotropic Shells and Plates," *Journal of the Aerospace Sciences*, Vol. 29, No. 8, Aug. 1962, pp. 969–975.

[3] Zienkiewicz, O. C., *The Finite Element Method in Structural and Continum Mechanics*, McGraw-Hill, New York, 1967.

[4] Przemieniecki, J. S., *Theory of Matrix Structural Analysis*, McGraw-Hill, New York, 1968.

[5] Rodden, W. P. et al., "Flutter and Vibration Analysis by a Collocation Method; Analytical Development and Computational Procedure," Rept. TDR-169(3230-11) TN-14, July 1963, Aerospace Corp., El Segundo, Calif.

[6] Theodorsen, T., "General Theory of Aerodynamic Instability and the Mechanism of Flutter," Rept. 496, 1935, NACA.

[7] Rodden, W. P. et al., "Aerodynamic Influence Coefficients by Incompressible Strip Theory; Analytical Development and Procedure for the IBM 7090 Computer," Rept. NOR-61-50, April 1961, NORAIR Div. of Northrop Corp., Hawthorne, Calif.

[8] Rodden, W. P. et. al., "Flexibility Matrix by Elastic Energy for Wings with an Elastic Axis; Analytical Development and Procedure for the IBM 7090 Computer," Rept. NOR-61-49, April 1961, NORAIR Div. of Northrop Corp., Hawthorne, Calif.

[9] Watkins, C. E., Runyan, H. L., and Woolston, D. S., "On the Kernal Function of the Integral Equation Relating the Lift and Downwash Distributions of Oscillating Finite Wings in Subsonic Flow," Rept. 1234, 1955, NACA.

[10] Moore, M. T. and Andrew, L. V., "Unsteady Aerodynamics for Advanced Configurations," Pt. IV, Rept. FDL-TDR-64-152, 1965, Air Force Flight Dynamics Lab.